Synergistic Effects of Mixed Metal Stearate, Calcium Carbonate Particles and Recycled Low Density Polyethylene on The Mechanical, Thermal and Structural Performance of Polyvinylchloride Blend.

Samira Maou (s.maou@univ-biskra.dz)
Universite Mohamed Khider de Biskra https://orcid.org/0000-0002-8309-5441
yazid Meftah
Universite Mohamed Khider de Biskra
ahmed Meghezzi
Universite Mohamed Khider de Biskra

Research Article

Keywords: PVC, r-LDPE, Thermal stabilizer, CaCO3, Density functional theory

Posted Date: March 3rd, 2022

DOI: https://doi.org/10.21203/rs.3.rs-1352930/v1

Abstract

Thermo-mechanical recycling process is the cheapest way to recover plastic wastes such as LDPE with lower ecological impact, thus, the target in this work is to achieve high performance microcomposites prepared from polyvinyl chloride (PVC), recycled low density polyethylene (r-LDPE), calcium carbonate ($CaCO_3$) and Calcium/Zinc stearate ($CaSt_2$/$ZnSt_2$). The effects of two ratios of thermal stabilizers with different concentrations, on the mechanical properties and thermal stability of PVC and PVC/r-LDPE (1:1) blend were studied. The samples were characterized using infrared spectroscopy (FTIR), mechanical tests, thermal analysis and scanning electron microscopy (SEM). The addition of 5 phr of $CaSt_2$:$ZnSt_2$ = 9:1 into PVC (MC4) seems to produce an optimum tensile strength and elongation at break values. In addition, it is highlighted that MC4 showed a high thermal stability. Moreover, the incorporation of r-LDPE into PVC makes the PVC matrix stronger and more stable than pure PVC which yields to high mechanical and thermal performances. Furthermore, an outstanding synergistic effect can be showed when heat stabilizer rich in calcium combined with $CaCO_3$ and r-LDPE. This PVC/r-LDPE blend as waste composite can be used in several industry fields. Finally, we used DFT calculation to elucidate the dehydrochlorination mechanism of PVC in presence of Ca and Zn stearate.

Introduction

The Novel industry technology influences positively on the performance of composite materials in the economic sector, especially thermoplastic polymers, blends and their composites [1]. For fast economic development and significant protection of the environment, recycled plastic waste technology is known as a clean energy source and plays a very important role in solid waste disposal [2, 3]. Agricultural plastic wastes (APW) is intrinsically difficult to recover and recycle in Algeria because the absence of APW systems and infrastructures [4, 5]. Polyvinylchloride (PVC) is one of the most important thermoplastic polymers used in industrial products, such as pipes, cables, food product container, construction applications, medical and electronic devices, due to high mechanical properties [6–8]. Lower thermal stabilization was observed for the PVC compared with other thermoplastic polymers such as : low density polyethylene (LDPE), high density polyethylene (HDPE), polypropylene (PP), polystyrene (PS) and polyethylene terephthalate (PET) due to dehydrochlorination reaction of PVC around 100°C [9]. The pyrolysis of PVC characterizes a two interesting steps : (1) initial degradation of PVC due to the first dehydrochlorination of PVC at low temperature, (2) final degradation due to strongly cracking and decomposition of the PVC at higher temperatures [10, 11]. To decrease the pure PVC degradation, it should be mixed with thermal stabilizers to produce plastic with high thermal performance used in several applications [12, 13]. Incorporation of thermal stabilizer into PVC can make the zipper decomposition more difficult at both low and high temperatures, in which the chlorine atom can be absorbed by heat stabilizer [14].The combination of commercial calcium stearate ($CaSt_2$) and zinc stearate ($ZnSt_2$) has attracted the attention of several researchers, in which $ZnSt_2$ can substitute labile chlorine atom of PVC chain forming a strong Lewis acid, $ZnCl_2$, which in turn can react with HCl to perform dehydrochlorination reaction. On the other side, HCl is absorbed by $CaSt_2$ to generate $CaCl_2$ and

fatty acid [15]. Moreover, calcium/zinc compounds can be considered as environmentally friendly thermal stabilizers compared with organo tin and lead compounds [16]. It is significant to develop new heat stabilizer of PVC that exhibited synergistic effect with commercial thermal stabilizers $CaSt_2/ZnSt_2$ [13, 17]. Li et al. found that new mixed Ca/Zn synthesized from tung oil fatty acid improved the thermal proprieties of PVC [18]. Moreover, Wang et al. studied the synergistic effect of tung-oil-based Ca/Zn and polyol in stabilizing polyvinylchloride [19]. The results show that the positive synergistic effect can be attributed to the hydroxyl and nitrogen groups of the heat stabilizers. In addition, Asawakosinchai et al. reported the 1,3-dimethyl-6-ami-nouracil (DAU) and eugenol are good thermal stabilizers of PVC compared with other heat stabilizers [20]. Recently, the synergistic effects of traditional heat stabilizer ($CaSt_2/ZnSt_2$) and Tung-oil-derived imide epoxidized ester (GEABTMI) on the thermal stabilization of PVC were successfully investigated by Wang et al. they found that the imide and epoxy functions of GEABTMI compound can scavenge free radicals and absorb HCl generated from PVC pyrolysis [21]. Li et al. studied the interesting performance of mechanical properties of the PVC composite reinforced with $CaCO_3$ nano-particles, which these particles considered as good dispersion agents in the PVC polymer system, and it can be an effective approach to resist the migration of plasticizer from the PVC [22]. It is well known that the addition of $CaCO_3$ fillers increase thermal stability of PVC polymer [23]. The results appeared that the $CaCO_3$ can absorb HCl to generate $CaCl_2$, CO_2 and H_2O [24]. Ahmad et al. investigated the synergistic effect of calcium carbonate ($CaCO_3$)/ layered double hydroxides (LDHs) on the thermal degradation of PVC [25]. Many researchers reported the incorporation of different polymers in PVC induced high thermal and mechanical performance [26–28]. Our previous experimental results revealed that thermal stability of the PVC/LDPE blend was improved significantly by increasing the LDPE loading to values above 50 wt% [29]. To the best of our knowledge there are no reports of degradation behavior of PVC, considering the synergistic effects of mixed metal stabilizers ($CaSt_2/ZnSt_2$) with different concentrations and different ratios of calcium/zinc stearates, Calcium carbonate ($CaCO_3$) as micro-filler and recycled low-density polyethylene (r-LDPE). In this paper, two ratios of calcium/zinc stearates metal Stabilizers, $CaCO_3$ particles and r-LDPE were added into PVC. This study investigates a new microcomposite based on PVC with high mechanical, thermal and morphological performance which can provide sufficient information to reveal the degradation process of PVC. Furthermore, we conducted density functional theory (DFT) calculations to elucidate the role of Ca-Zn in thermal stability of PVC.

Experimental

Materials

The recycled LDPE Films (melting point: 128°C, Density: 0.9555 g/cm^{-3}, and MFI: 0.92 (g/10min,190 ^{o}C/2.16kg)) used in the current study were collected from agricultural plastic waste (greenhouse) in Biskra, Algeria. An amorphous PVC white powder (4000M, K-value = 67–72) was purchased from the “Enterprise National de Pétrochimie (ENIP)”, Skikda, Algeria. Calcium stearate ($CaSt_2$, Ca content: 6.6–7.4%), zinc stearate ($ZnSt_2$, Zn content: 10–12%), and calcium carbonate ($CaCO_3$, 2500 mesh) were

obtained from Nanjing OMYA Fine Chemical Ind. Co. Ltd. (Nanjing China). Bis (2-ethylhexyl) terephthalate (DOP, 98%) was obtained from Shanxi Sanwei Group Co., Ltd. Mixed Metal Stabilizers Calcium / Zinc stearate were prepared in the form of ($CaSt_2$: $ZnSt_2$ = 9:1 and $CaSt_2$: $ZnSt_2$ = 1:9).

Fabrication of microcomposites

Recycled LDPE was washed with detergent and water. All materials were dried in an oven at 80℃ for 12 hours before blending to remove humidity. PVC and PVC/r-LDPE (1:1) microcomposites using different concentrations of mixed metal stabilizers and calcium carbonate were extruded using the twin screw extruder, type MSH, at a processing temperature of 175°C, screw speed of 50 rpm for 10 min from the feed zone to die zone. All different samples are summarized in the Table 1, the samples obtained after extruding were cooled at room temperature and then it was pressed into a square mold with dimension of 200 x 200 x1mm, using a heated hydraulic press for 7 min at 170°C with 200-bar pressure. After cooling with water system to room temperature, the sample was cut off in altered form by the (Computer numerical control) CNC milling machine, before carrying out different characterizations.

Table 1
Different composition of the PVC and PVC/LDPE microcomposites.

Sample	PVC (phr)	LDPE (phr)	$CaCO_3$ (phr)	Heat stabilizer [(a)&(b)] (phr)	Plasticizer DOP (phr)
MC0	100	-	20	-	25
MC1	100	-	20	2[a]	25
MC2	100	-	20	2[b]	25
MC3	100	-	20	5[a]	25
MC4	100	-	20	5[b]	25
MC5	100	-	20	10[a]	25
MC6	100	-	20	10[b]	25
MC7	100	100	20	2[a]	25
MC8	100	100	20	2[b]	25
MC9	100	100	20	5[a]	25
MC10	100	100	20	5[b]	25
MC11	100	100	20	10[a]	25
MC12	100	100	20	10[b]	25
[(a)]Attribute to the $CaSt_2$: $ZnSt_2$ = 1:9 and [(b)] attribute to the $CaSt_2$: $ZnSt_{2=}$ 9:1 heat stabilizer.					

Table 1 Different composition of the PVC and PVC/r-LDPE microcomposites

Characterizatio n

Fourier transform infrared spectroscopy (FTIR)

The structural analysis of the PVC and PVC / r-LDPE microcomposite samples were carried out by Fourier Transform Infrared Spectroscopy Vertex 70v FTIR (Bruker Company, Billerica, MA, USA) coupled with ATR Golden Gate Diamond. The Samples were measured from 4000 to 400 cm^{-1} with a 4 cm^{-1} spectrum resolution to obtain FTIR spectra.

Mechanical tests

The mechanical tests were conducted on samples with dimension of 40 × 10× 1 mm at ambient conditions, using a mechanical testing machine (Zwick / Roell, ISO 527, Germany) at a crosshead speed

of 10 mm/min using ASTM D638. The standard dimension was 40 mm in length, 10 mm in width, and 1mm in thickness. Each tensile sample was performed five times to report the average value.

Heat ageing test. The samples were heated in air oven at 100 ± 1°C for 360 h (15 days), the heat ageing of tensile strength, young's modulus and elongation-at-break values of the samples was carried out in accordance with ASTM D3045 to evaluate changes in the mechanical properties after ageing.

Investigation of initial thermal stabilization for microcomposites.

Congo Red Test

10.0 g of each PVC sample was put into an airtight tube and immersed in oil bath at 180°C refer to the GB/T 2917.1–2002 standard, furthermore, the PVC samples were controlled by Congo red paper and the thermal stability time was recorded when the color of the paper turned blue. The Congo red test was executed three times and an average value was reported.

Discoloration test

PVC and PVC/r-LDPE samples were cut into sheets having dimensions of 15.0 mm×15.0 mm ×2.0 mm according to the GB/T 9349 − 2002 standard. The samples were moved onto the ceramic plate in temperature-controlled oven (V 50 e, Prolabo) at 180°C, after that the samples were scanned every 10 min using (Epson Perfection V19) to evaluate the PVC discoloration during heating.

Thermogravimetric analysis (TGA and DTG). The TGA and DTG results of the microcomposites were obtained by using SDT Q600 (TGA/DSC simultaneous thermo gravimetric analyzer and differential scanning calorimeter) from TA Instruments under N_2 atmosphere with a heating rate of 10°C/min using 3 to 5 mg of the sample was analyzed. The temperature range was from 25 to 600°C.

Scanning electron microscopy (SEM). The morphology of the microcomposites was examined using scanning electron microscope (SEM) (JEOL JSM 6460LV) with an accelerating voltage of 20 kv. The samples were soaked in liquid nitrogen before fracturing and then were covered with a thin gold layer by sputtering using EDWARDS scan-coat on the surface and the cross-sections.

Calculation details. All the calculations were conducted by using the Gaussian 09 program package [30], we used hybrid functional M06-2X [31], because several theoretical studies of polymer pyrolysis reported that this functional is more viable in comparison with B3LYP [32–34], to reduce the computational cost, a 4-carbon PVC molecule and the polar part of thermal stabilizers $CaSt_2$ and $ZnSt_2$, were employed as a model reactants. Geometries of the reactants (R1, R2), transition states (TS1, TS2), and products (P1, P2) were optimized at M06-2X/6–31 + + G(d,p) level of theory. Frequencies were computed for all stationary points and used to compute the free energies at 298 K and 1 bar. Finally, we performed IRC calculation to confirm the connection between products and reactants.

Results And Discussion

Structure characterization of the PVC and PVC/r-LDPE microcomposites

FTIR tests were conducted to investigate and clarify the modifications in the functional groups of the microcomposites with different heat stabilizer ratios after the heat ageing at 100°C for 168 hours. From the FTIR spectra depicted in Fig. 1 and Fig. 2, the characteristic bands of PVC and PVC/r-LDPE microcomposites are well shown and the assignments of these bands are in line with those provided by several researchers corresponding with composites based on PVC [35–37].

Figure 1 FTIR spectra of PVC microcomposites exposed to thermal ageing for t = 360 h under temperature T = 100°C:(a) OH water group superposed region, (b) CO carbonyl group superposed region

Figure 2 FTIR spectra of PVC/r-LDPE microcomposites exposed to thermal ageing for 360 h under temperature T = 100°C : (a) OH water group region, (b) CO carbonyl group region

The peaks in the region 2940–2960 cm^{-1} correspond to symmetric stretching C-H in the adjacent CH-Cl, but the peak at 2849 cm^{-1} in PVC/r-LDPE microcomposites is attributed to the asymmetric stretching, of C-H in -CH3 groups and in -CH2- groups. The peaks in the range 800–870 cm^{-1} can be attributed to the calcium carbonate group $CaCO_3$. Moreover, the asymmetric stretching of C-Cl can be related to the peaks in the range of 610–730 cm^{-1}. Furthermore, the weak bands around 3620 and 3660 cm^{-1} in Fig. 1a and Fig. 2a, attributed to the hydroxyl group OH stretch of the water phase may result from adsorption of HCl by $CaCO_3$ particles. A strong peak at 1732 cm^{-1} in Fig. 1b and Fig. 2b is attributed to C = O stretch presented in DOP structure and it is probably due to the oxidation process during heat ageing test. Finally, we can conclude that PVC and PVC/r-LDPE microcomposites with different heat stabilizers concentrations are not significantly affected by thermal ageing at 100°C, as shown in Fig. 1 and Fig. 2. The difference of FTIR peaks between PVC and PVC/r-LDPE micro composites are visible in the superposed intensity and shape of characteristic bands represented above.

Mechanical properties of the PVC and PVC/r-LDPE microcomposites

The Tensile strength, Elongation at break and Young's modulus results of PVC and PVC/r-LDPE microcomposites before and after ageing are displayed in Fig. 3a and b and Table 2. It showed that pure PVC gets more brittle, as compared with the PVC matrix contained heat stabilizers, $CaCO_3$, and r-LDPE polymer, which these additives make the material more mechanically stable.

Table 2
The mechanical results before and after heat ageing of PVC and PVC/LDPE microcomposites.

sample	Before ageing			After ageing		
	Tensile Strength	Young's Modulus	Elongation at break	Tensile Strength	Young's Modulus	Elongation at break
	σ (MPa)	E (MPa)	ε (%)	σ (MPa)	E (MPa)	ε (%)
MC0	15,55 ± 0,8	30,33 ± 1,1	301,02 ± 15,2	12,2 ± 0,5	20,4 ± 1,3	250,5 ± 16,2
MC1	17,38 ± 0,5	40,24 ± 0,9	340,3 ± 20	15,6 ± 1	37,23 ± 0,9	300,09 ± 17,9
MC2	18 ± 0,7	44,23 ± 0,8	344,14 ± 21	17,6 ± 0,6	40,2 ± 1,4	305,76 ± 18,9
MC3	18,5 ± 0,8	56,41 ± 1	351,5 ± 19,6	17,9 ± 0,9	52,7 ± 1,6	320 ± 14
MC4	19,6 ± 1	60,32 ± 1,3	381,62 ± 19	19 ± 0,7	56,4 ± 0,6	360,34 ± 16,5
MC5	16,84 ± 1	36,03 ± 0,9	313,05 ± 22,5	15 ± 1,5	31,1 ± 0,7	287,91 ± 16,5
MC6	16,5 ± 0,4	42,27 ± 1,2	314,11 ± 17	15,9 ± 0,3	39,2 ± 1,2	290,7 ± 16,5
MC7	6,06 ± 0,5	95.14 ± 5,1	11,52 ± 0,6	5,50 ± 0,4	90,26 ± 4,9	10,4 ± 0,5
MC8	5,98 ± 0,3	99.20 ± 4	13,72 ± 0,9	5,60 ± 0,4	96,22 ± 5,7	12,5 ± 0,8
MC9	5,38 ± 0,3	115.33 ± 8,3	17,06 ± 12	4,98 ± 0,2	110 ± 8,6	16,12 ± 1,1
NC10	7.00 ± 0,5	130.19 ± 9	18,11 ± 1,4	6,80 ± 0,3	127,21 ± 10	17,5 ± 1
MC11	3,73 ± 0,2	80.20 ± 7,2	11 ± 0,5	3,63 ± 0,5	75,03 ± 5	10 ± 0,7
MC12	4,61 ± 0,4	65.44 ± 5,5	13,3 ± 11	4,58 ± 0,3	62 ± 3,9	12,6 ± 0,9

Figure 3a shows the variation of tensile behaviors of PVC microcomposites at different heat stabilizers ratios. The mechanical performance is remarkably decreased in the sample without thermal stabilizer MC0 after ageing. In addition, the sample MC4 exhibit better mechanical performance than the pure PVC and other samples, before and after ageing. It revealed that the optimum concentration of mixed stearate $CaSt_2$: $ZnSt_2$ = 9 :1 for the highest tensile strength, elongation at break and young's modulus is 5 phr, this concentration probably leads to the good dispersion of $CaSt_2$ particles in PVC microcomposite. From a mechanical point of view, we can also see that 2 phr of thermal stabilizers MC1 and MC2 are slightly better than 10 phr, MC5 and MC6 with little favor of heat stabilizer with a high concentration of calcium, due to the interaction between the polar ends of Calcium stearate and the somewhat polar PVC chains [38].

Figure 3 Evolution of the mechanical properties of PVC and PVC/r-LDPE microcomposites before and after heat ageing

Figure 3b represents the influence of r-LDPE on the mechanical properties of the PVC microcomposites with 2, 5 and 10 phr of mixed metal stabilizers. It can be observed that the incorporation of r-LDPE into PVC decreases the tensile strength and elongation at break when it is compared with PVC micro composites. This deterioration is due to the crystalline structure part of the macromolecular chain of r-LDPE polymer and which makes the PVC polymer loses partially its flexibility [39]. On the other hand, Young's Modulus values are doubly increased after addition of r-LDPE into PVC microcomposites. In addition, MC10 exhibits better mechanical properties than other samples, before and after ageing. In addition, it can be seen that the incorporation of r-LDPE enhances the mechanical stability of the PVC polymer after heat ageing. Hence, during the thermal treatment the PVC and short-chain r-LDPE radicals react to produce r-LDPE-g-PVC copolymers [26]. The mechanical properties of microcomposites based on PVC become higher with increasing the content of $CaSt_2$.

Table 2 The mechanical results before and after heat ageing of PVC and PVC/r-LDPE microcomposites

Effects of thermal stabilizers and r-LDPE on stabilizing PVC microcomposites

Figure 4a and b shows the results of Thermal stability time (Congo red test) of PVC microcomposites at 180°C and discoloration photos of PVC and PVC/r-LDPE microcomposites at 180°C for 110 min of three different concentrations of thermal stabilizers with ($CaSt_2$: $ZnSt_2$ = 9:1 and $CaSt_2$: $ZnSt_2$ = 1:9), respectively. As shown in Fig. 4a, the PVC microcomposites MC4 and MC6, when the thermal stabilizer is rich in calcium, it can relatively improve the thermal stability time (t = 160 min) [40, 41]. Whereas, in Fig. 4b thermal stability increased with increasing heat stabilizer concentrations and delayed the discoloration of PVC samples with a significantly resistance to discoloration of PVC/r-LDPE samples MC10 and MC12 which the incorporation of r-LDPE into PVC showed much better antidiscoloration compared with PVC microcomposites. In addition, the samples rich in Zinc stearate MC1, MC3, MC5, MC7, MC9, and MC11 quickly turned to dark color, the reason is that $ZnSt_2$ can remove initial coloration by substituting labile chlorine atoms from the PVC chain [42]. However, the heat stabilizer rich in calcium stearate increases the PVC stabilization time due to the inhibition of $ZnCl_2$ which is responsible of dehydrochlorination process [43]. As is known, $CaSt_2$ could react with $ZnCl_2$ to regenerate $ZnSt_2$ and $CaCl_2$ via ester exchange reaction. On the other side, a detailed computational study is required to understand the dehydrochlorination process in presence of $CaSt_2$ and $ZnSt_2$.

Figure 4 (a) Thermal stability time (Congo red test) of PVC microcomposites at 180°C. (b) Discoloration photos of PVC and PVC/r-LDPE microcomposites at 180°C for 110 min

Thermal properties of the PVC and PVC/r-LDPE microcomposites

The thermo-gravimetric curves of PVC and PVC/r-LDPE microcomposite with different metal mixed heat stabilizers ratios are plotted in Fig. 5a-d. The important temperatures and different thermal degradation

levels of PVC and PVC/r-LDPE microcomposites are summarized in Table 3. As shown in the TGA graphs, thermal degradation of PVC and PVC/r-LDPE occurred in two major steps.

Table 3
Interested decomposition temperatures and weight loss levels of PVC and PVC/LDPE microcomposites

Sample	Decomposition temperature							
	T^{Onset} (°C)	$T^{10\%}$ (°C)	First stage			Second stage		
	Tmax (°C)	Mass loss (%)	T_{range} /(°C)	Tmax (°C)	Mass loss (%)	T_{range} /(°C)		
MC1	277.28	285.36	399.54	54.07	277–343	468.30	66.50	442–490
MC2	278.72	286.43	301.22	5 3.10	278–350	464.63	67.50	440–493
MC3	281.13	284.10	288.00	54.00	281–335	474.49	66.30	441–494
MC4	285.55	291.29	302.91	51.09	286–355	473.75	64.21	444–498
MC5	283.30	292.24	296.23	52.51	283–330	470.27	63.00	445–502
MC6	284.61	295.56	300.32	52.23	284–339	470.02	62.10	446–501
MC7	283.52	289.83	290.20	31.00	283–315	490.6	67.40	468–505
MC8	284.48	293.53	305.80	34.00	285–317	491.01	70.50	463–508
MC9	281.00	286.72	290.03	31.45	281–323	490.55	64.60	470–509
MC10	290.20	297.72	304.82	31.35	290–325	492.51	63.50	474–511
MC11	277.22	285.44	292.65	31.90	276–322	490.06	68.55	471–508
MC12	286.42	296.06	300.19	31.50	286–324	492.23	64.85	472–510

Figure 5a and b shows the first degradation of PVC begins around 277°C with remarkably lose weight which is attributed to the dehydrochlorination of PVC and the second degradation is related to the scission of polyene sequences [10, 44].The onset degradation temperatures of PVC microcomposites are in the range of 276–290˚C. It is observed that the samples MC1 and MC2 have lower decomposition

temperatures as compared to any other PVC microcomposite, due to a small amount of heat stabilizer incorporated in the PVC matrix, moreover, as long as the heat stabilizer is increased, the PVC degradation is delayed significantly in the MC4, MC5 and MC6 samples, in which MC4 sample shifts to higher values. As expected, the thermal stability of samples containing high calcium concentration are much better than samples with high zinc concentration into mixed metal stabilizer, due to the ability of $CaSt_2$ to absorb more HCl which indeed leads to much less the dehydrochlorination, and more stability of PVC microcomposites [45].

Figure 5 (a, b) TGA and DTG curves of PVC and (c, d) TGA and DTG curves of PVC/r-LDPE microcomposites

Figure 5c and d represented the influencing of r-LDPE on the thermal degradation of PVC, which plays the same role as heat stabilizer. Similarly to PVC degradation, it can be seen that the optimum concentration of mixed stearate $CaSt_2$: $ZnSt_2$ = 9 :1 for the degradation of PVC/r-LDPE microcomposite is 5 phr, in addition, it can be concluded that the incorporation of r-LDPE into PVC enhances the values of onset degradation temperatures up to 290°C and retards the degradation process [36], accordingly to the mechanism which was proposed by Thongpin et al. [46], and Sombatsompop et al. [26], in particular through the starting of the initiation co-cross-linking process which results in macro-radical recombination reactions which lead to producing more short chains, PVC grafted with r-LDPE at high temperatures.

Table 3 Interested decomposition temperatures and weight loss levels of PVC and PVC/r-LDPE microcomposites

Fracture surface morphology of the PVC and PVC/r-LDPE microcomposites

Figure 6 presents SEM micrographs for fracture surfaces of PVC and PVC/r-LDPE with $CaCO_3$ particles and $CaSt_2$: $ZnSt_2$ = 9:1. Figure 6a and c shows that the hydrophilic $CaCO_3$ micro-particles were highly aggregated in the PVC matrix, with several voids present, leading to a decrease in the interfacial adhesion between $CaCO_3$ particles and PVC matrix [47]. Figure 6b and d reveals a good compatibility between $CaCO_3$ microparticles and PVC/r-LDPE mixtures compared with PVC matrix, due to the well distribution of $CaCO_3$ in the blend. As the PVC was blended with r-LDPE, the $CaCO_3$ were well dispersed in the PVC/r-LDPE blend, which led to a strong interfacial interaction between PVC/r-LDPE and $CaCO_3$ microparticles [48]. These findings are in accordance with the mechanical behaviors of microcomposites.

Figure 6 SEM images of the fracture surfaces of (a,c) MC4 and (b,d) MC10 microcomposites

DFT calculation results

Geometries optimization of reactants, transitions state and products were depicted in Fig. 7a. PVC polymer, may be regarded as polar, interacted with the polar part of thermal stabilizers. The strong

hydrogen bond between H of PVC and O of $Cast_2$ and $Znst_2$ is 2.29 and 2.35 Å, respectively, reveals the stability of reactants. In addition, Ca and Zn formed electrostatic bond with Cl by 2.87 and 2.49 Å, respectively. The simultaneous transfer of the chlorine and the hydrogen to the thermal stabilizers leads to the formation of unsaturated groups in PVC and takes place via TS1 and TS2 which lies 29.6 and 25.0 kcal/mol, respectively, above reactants. The free energy profiles of the dehydrochlorination process are displayed in Fig. 7b, we found that dehydrochlorination process can occur via a concerted mechanism with four- member ring transition state and the free activation energy with $ZnSt_2$ is smaller than that with $CaSt_2$. Our DFT results are consistent with previous theoretical and experimental results [45, 49].

Figure 7 (a) Optimized geometries of reactants, transition states and products for the thermal dehydrochlorination of PVC with different thermal stabilizers. Distance given in A°.Atom color code: H in white, C in grey, Cl in green, O in red, Ca in yellow and Zn in blue and (b) Relative free energies of the dehydrochlorination process with (blue) $CaSt_2$ and (red) $ZnSt_2$ at the M06-2X/6–31 + + G(p,d) level

Conclusions

This work highlights the importance of different additives, such as mixed metal calcium/zinc stearate, $CaCO_3$ particles, and r-LDPE with their positive effects to enhancing the polyvinylchloride (PVC) properties. The $CaSt_2/ZnSt_2$ stearate as heat stabilizer does not affect alone on PVC degradation and mechanical properties, but the addition of r-LDPE in the PVC helps to upgrade the performance of the latter to be used in several fields. The optimum ratio of ($CaSt_2$: $ZnSt_2$ = 9:1) was 5phr which can yield good thermal stability and high mechanical performance of PVC microcomposite before and after the heat ageing test. r-LDPE as a thermoplastic polymer, with 50 phr content, exhibited the best young modulus before and after heat ageing, and confirmed the ability to be a highly effective compound to protecting the thermal stability of the PVC. Thermal analysis revealed the excellent synergistic effects of $CaCO_3$, heat stabilizer rich in calcium and r-LDPE for more thermal stability of PVC polymer.

SEM micrographs show that the $CaCO_3$ microparticles is well dispersed in the PVC/r-LDPE blend, which leads to a strong interfacial interaction between PVC and r-LDPE. Finally, DFT calculation revealed that dehydrochlorination process can occur by the simultaneous transfer of the chlorine and the hydrogen to the thermal stabilizers via a concerted mechanism with four- member ring transition state with a low free energy barrier in favor to $ZnSt_2$. This can help polymerists to design new thermal stabilizers for PVC.

Declarations

Acknowledgements

The authors are grateful to the staff of plastic laboratory of (Entreprise des Industries du Câble ENICAB), Biskra, Algeria, for suppling the PVC polymer and their additives of this work, the (Centre de Recherche Scientifique & Technique en Analyse Physico-Chimiques CRAPC), Tipaza, Algeria, for thermal analysis.

The authors are also thankful acknowledgments to Dr. Antoine Kervoelen and Anthony Magueresse for supporting this experimental work by the characterization methods.

References

1. Yao J, Zhou Z, Zhou H (2019) Highway engineering composite material and its application. Highw Eng Compos Mater Its Appl 1–163.
2. Kumagai S, Hirahashi S, Grause G, et al (2018) Alkaline hydrolysis of PVC-coated PET fibers for simultaneous recycling of PET and PVC. J Mater Cycles Waste Manag 20:439–449.
3. Suresh SS, Mohanty S, Nayak SK (2020) Effect of recycled poly(vinyl chloride) on the mechanical, thermal and rheological characteristics of recycled poly(methyl methacrylate). J Mater Cycles Waste Manag 22:698–710.
4. Briassoulis D, Hiskakis M, Babou E (2013) Technical specifications for mechanical recycling of agricultural plastic waste. Waste Manag 33:1516–1530.
5. Guermoud N, Ouadjnia F, Abdelmalek F, et al (2009) Municipal solid waste in Mostaganem city (Western Algeria). Waste Manag 29:896–902.
6. Liu Y, Zhou C, Li F, et al (2020) Stocks and flows of polyvinyl chloride (PVC) in China: 1980-2050. Resour Conserv Recycl 154: 104584.
7. Ye L, Qi C, Hong J, Ma X (2017) Life cycle assessment of polyvinyl chloride production and its recyclability in China. J Clean Prod 142:2965–2972.
8. Ali I, Yang W, Li X, et al (2020) Highly electro-responsive plasticized PVC/FMWCNTs soft composites: A novel flex actuator with functional characteristics. Eur Polym J 126:109556.
9. Yu J, Sun L, Ma C, et al (2016) Thermal degradation of PVC: A review. Waste Manag 48:300–314.
10. Abbas-Abadi MS (2021) The effect of process and structural parameters on the stability, thermo-mechanical and thermal degradation of polymers with hydrocarbon skeleton containing PE, PP, PS, PVC, NR, PBR and SBR. J Therm Anal Calorim 143:2867–2882.
11. Saeedi M, Ghasemi I, Karrabi M (2011) Thermal degradation of poly(vinyl chloride): effect of nanoclay and low density polyethylene content. Iran Polym J 20:423–432
12. Balköse D, Gökçel Hİ, Göktepe SE (2001) Synergism of Ca/Zn soaps in poly(vinyl chloride) thermal stability. Eur Polym J 37:1191–1197.
13. Zhang M, Han W, Hu X, et al (2020) Pentaerythritol p-hydroxybenzoate ester-based zinc metal alkoxides as multifunctional antimicrobial thermal stabilizer for PVC. Polym Degrad Stab 181:109340.
14. Liu Y Bin, Liu WQ, Hou MH (2007) Metal dicarboxylates as thermal stabilizers for PVC. Polym Degrad Stab 92:1565–1571.
15. Wang M, Song X, Jiang J, et al (2017) Binary amide-containing tung-oil-based Ca/Zn stabilizers: effects on thermal stability and plasticization performance of poly(vinyl chloride) and mechanism of thermal stabilization. Polym Degrad Stab 143:106–117.

16. Korkusuz, Tüzüm Demir AP (2020) Evaluation of the thermal stabilization behavior of hydrotalcite against organic stabilizers for plasticized PVC films. Polym Bull 77:4805–4831.
17. Ye F, Ye Q, Zhan H, et al (2019) Synthesis and study of zinc orotate and its synergistic effect with commercial stabilizers for stabilizing poly(vinyl chloride). Polymers (Basel) 11:194.
18. Li M, Zhang J, Xin J, et al (2017) Design of green zinc-based thermal stabilizers derived from tung oil fatty acid and study of thermal stabilization for PVC. J Appl Polym Sci 134:16–20.
19. Wang M, Song X, Jiang J, et al (2017) Excellent hydroxyl and nitrogen rich groups-containing tung-oil-based Ca/Zn and polyol stabilizers for enhanced thermal stability of PVC. Thermochim Acta 658:84–92.
20. Asawakosinchai A, Jubsilp C, Mora P, Rimdusit S (2017) Organic Heat Stabilizers for Polyvinyl Chloride (PVC): A Synergistic Behavior of Eugenol and Uracil Derivative. J Mater Eng Perform 26:4781–4788.
21. Wang M, Li S, Ding H, et al (2020) Construction of efficient tung-oil-based thermal stabilizers bearing imide and epoxy groups for PVC. New J Chem 44:4538–4546.
22. Li X, Xiao Y, Wang B, et al (2012) Effects of poly(1,2-propylene glycol adipate) and nano-CaCO3 on DOP migration and mechanical properties of flexible PVC. J Appl Polym Sci 124:1737–1743.
23. Tawancy HM, Hassan M (2016) On the Degradation Mechanism of Low-Voltage Underground Cable with Poly(Vinyl Chloride) Insulation. J Mater Eng Perform 25:2288–2295.
24. Liu P, Zhao M, Guo J (2006) Thermal stabilities of poly(vinyl chloride)/calcium carbonate (PVC/CaCO3) composites. J Macromol Sci Part B Phys 45 B:1135–1140.
25. Ahamad A, Patil CB, Gite V V., Hundiwale DG (2013) Evaluation of the synergistic effect of layered double hydroxides with micro- and nano-CaCO3 on the thermal stability of polyvinyl chloride composites. J Thermoplast Compos Mater 26:1249–1259.
26. Sombatsompop N, Sungsanit K, Thongpin C (2004) Structural changes of PVC in PVC/LDPE melt-blends: Effects of LDPE content and number of extrusions. Polym Eng Sci 44:487–495.
27. Yuan Z, Zhang J, Zhao P, et al (2020) Synergistic Effect and Chlorine-Release Behaviors during Co-pyrolysis of LLDPE, PP, and PVC. ACS Omega 5:11291–11298.
28. Maou S, Meghezzi A, Grohens Y, et al (2021) Industrial Crops & Products Effect of various chemical modifications of date palm fibers (DPFs) on the thermo-physical properties of polyvinyl chloride (PVC) – high-density polyethylene (HDPE) composites. Ind Crop Prod 171:113974.
29. Maou S, Meghezzi A, Nebbache N, Meftah Y (2019) Mechanical, morphological, and thermal properties of poly(vinyl chloride)/low-density polyethylene composites filled with date palm leaf fiber. J Vinyl Addit Technol 25:E88–E93.
30. M.J. Frisch, G.W. Trucks, H.B. Schlegel, G.E. Scuseria, M.A. Robb, J.R. Cheeseman, G. Scalmani, V. Barone, B. Mennucci, G.A. Petersson, H. Nakatsuji, M. Caricato, X. Li, H.P. Hratchian, A.F. Izmaylov, J. Bloino, G. Zheng, J.L. Sonnenberg, M. Hada, M. Ehara, K. Toyota, R. Fukuda, J. Hasegawa, M. Ishida, T. Nakajima, Y. Honda, O. Kitao, H. Nakai, T. Vreven, J.A. Montgomery Jr., J.E. Peralta, F. Ogliaro, M. Bearpark, J.J. Heyd, E. Brothers, K.N. Kudin, V.N. Staroverov, T. Keith, R.Kobayashi, J. Normand, K.

Raghavachari, A. Rendell, J.C. Burant, S.S. Iyengar, J. Tomasi, M. Cossi, N. Rega, J.M. Millam, M. Klene, J.E. Knox, J.B. Cross, V. Bakken, C. Adamo, J. Jaramillo, R. Gomperts, R.E. Stratmann, O. Yazyev, A.J. Austin, R. Cammi, C. Pomelli, J.W. Ochterski, R.L. Martin, K. Morokuma, V.G. Zakrzewski, G.A. Voth, P. Salvador, J.J. Dannenberg, S. Dapprich, A.D. Daniels, O. Farkas, J.B. Foresman, J.V. Ortiz, J. Cioslowski, D.J. Fox, Gaussian 09, Revision D.01, Gaussian, Inc., Wallingford CT, 2013.

31. Zhao Y, Truhlar DG (2008) Density Functionals with Broad Applicability in Chemistry. Acc Chem Res 41:157–167.
32. Huang J, He C, Li X, et al (2018) Theoretical studies on thermal degradation reaction mechanism of model compound of bisphenol A polycarbonate. Waste Manag 71:181–191.
33. Huang J, Li X, Zeng G, et al (2018) Thermal decomposition mechanisms of poly(vinyl chloride): A computational study. Waste Manag 76:483–496.
34. Huang J, Li X, Meng H, et al (2020) Studies on pyrolysis mechanisms of syndiotactic polystyrene using DFT method. Chem Phys Lett 747:137334.
35. Wu J, Chen T, Luo X, et al (2014) TG/FTIR analysis on co-pyrolysis behavior of PE, PVC and PS. Waste Manag 34:676–682.
36. Zhu HM, Jiang XG, Yan JH, et al (2008) TG-FTIR analysis of PVC thermal degradation and HCl removal. J Anal Appl Pyrolysis 82:1–9.
37. Wang Z, Xie T, Ning X, et al (2019) Thermal degradation kinetics study of polyvinyl chloride (PVC) sheath for new and aged cables. Waste Manag 99:146–153.
38. Rabinovitch EB, Lacatus E, Summers JW (1984) The lubrication mechanism of calcium stearate/paraffin wax systems in PVC compounds. J Vinyl Technol 6:98–103.
39. Xu C, Fang Z, Zhong J (1993) Study on compatibilization-crosslinking synergism in PVC/LDPE blends. Die Angew Makromol Chemie 212:45–52.
40. Shi Y, Chen S, Ma M, et al (2016) Highly efficient and antibacterial zinc norfloxacin thermal stabilizer for poly(vinyl chloride). RSC Adv 6:97491–97502.
41. Wu B, Wang Y, Chen S, et al (2018) Stability, mechanism and unique “zinc burning” inhibition synergistic effect of zinc dehydroacetate as thermal stabilizer for poly(vinyl chloride). Polym Degrad Stab 152:228–234.
42. Liu Z, Fan J, Feng J, et al (2020) Study on the use of rare earth stabilizer as poly(vinyl chloride) stabilizer. J Vinyl Addit Technol 26: 536–547.
43. Jiang P, Song Y, Dong Y, et al (2013) Zinc glycerolate with lanthanum stearate to inhibit the thermal degradation of poly(vinyl chloride). J Appl Polym Sci 127:3681–3686.
44. Chen J, Liu Z, Nie X, Zhou Y, Jiang J, Murray RE (2018) Plasticizers derived from cardanol: synthesis and plasticization properties for polyvinyl chloride(PVC). J Polym Res 25:128–114.
45. González-Ortiz LJ, Arellano M, Jasso CF, et al (2005) Thermal stability of plasticized poly(vinyl chloride) compounds stabilized with pre-heated mixtures of calcium and/or zinc stearates. Polym Degrad Stab 90:154–161.

46. Thongpin C, Santavitee O, Sombatsompop N (2006) Degradation mechanism and mechanical properties of PVC in PVC-PE melt blends: Effects of molecular architecture, content, and MFI of PE. J Vinyl Addit Technol 12:115–123.
47. Sun S, Li C, Zhang L, et al (2006) Interfacial structures and mechanical properties of PVC composites reinforced by CaCO3 with different particle sizes and surface treatments. Polym Int 55:158–164.
48. Pham HNT, Nguyen VT (2020) Effect of calcium carbonate on the mechanical properties of polyethylene terephthalate/polypropylene blends with styrene-ethylene/butylene-styrene. J Mech Sci Technol 34:3925-3930.
49. Wang Y, Wang X, Liu L, Peng X (2009) Theoretical study on the thermal dehydrochlorination of model compounds for poly(vinyl chloride). J Mol Struct THEOCHEM 896:34–37.

Figures

Figure 1

FTIR spectra of PVC microcomposites exposed to thermal ageing for t= 360 h under temperature T=100°C:(a) OH water group superposed region, (b) CO carbonyl group superposed region

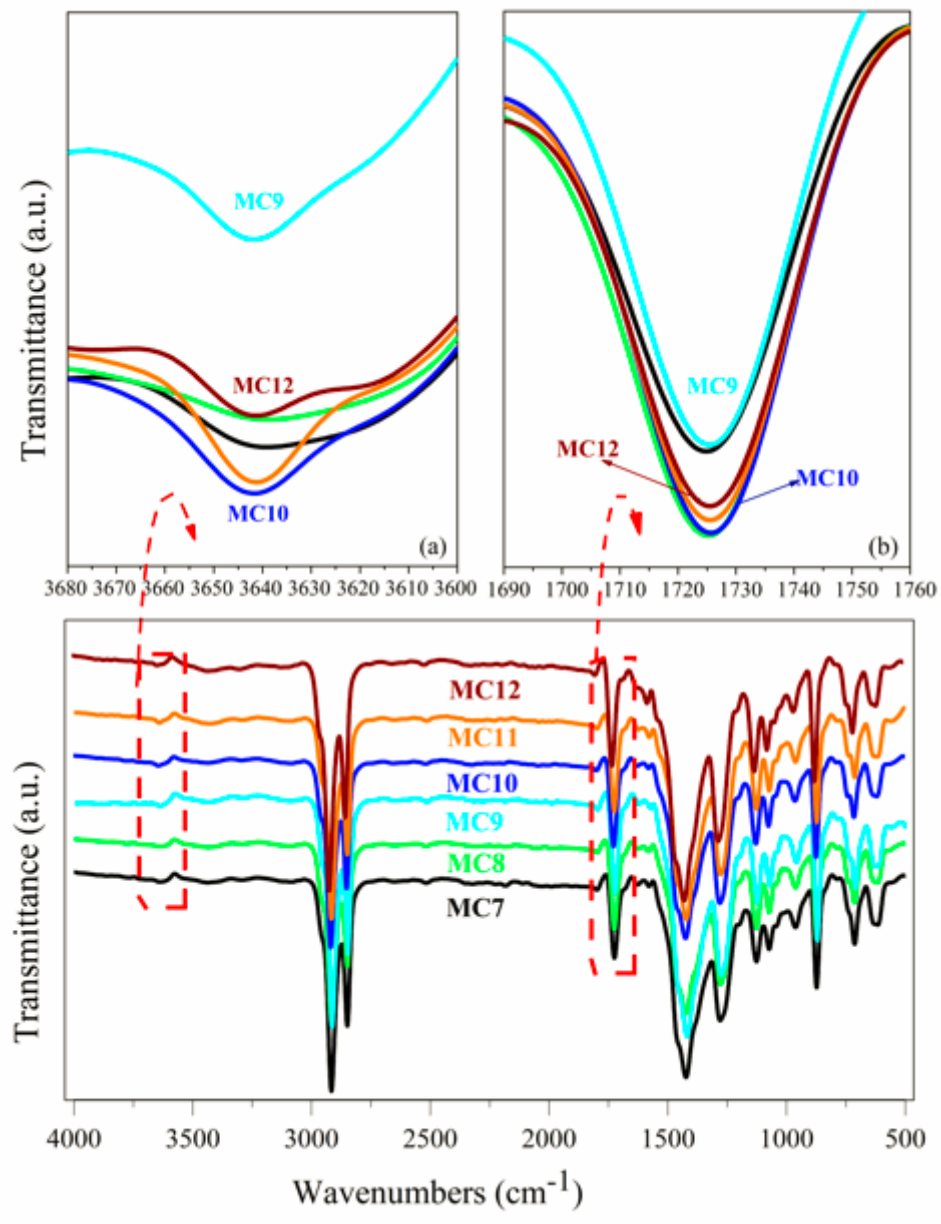

Figure 2

FTIR spectra of PVC/r-LDPE microcomposites exposed to thermal ageing for 360 h under temperature T=100°C : (a) OH water group region, (b) CO carbonyl group region

Figure 3

Evolution of the mechanical properties of PVC and PVC/r-LDPE microcomposites before and after heat ageing

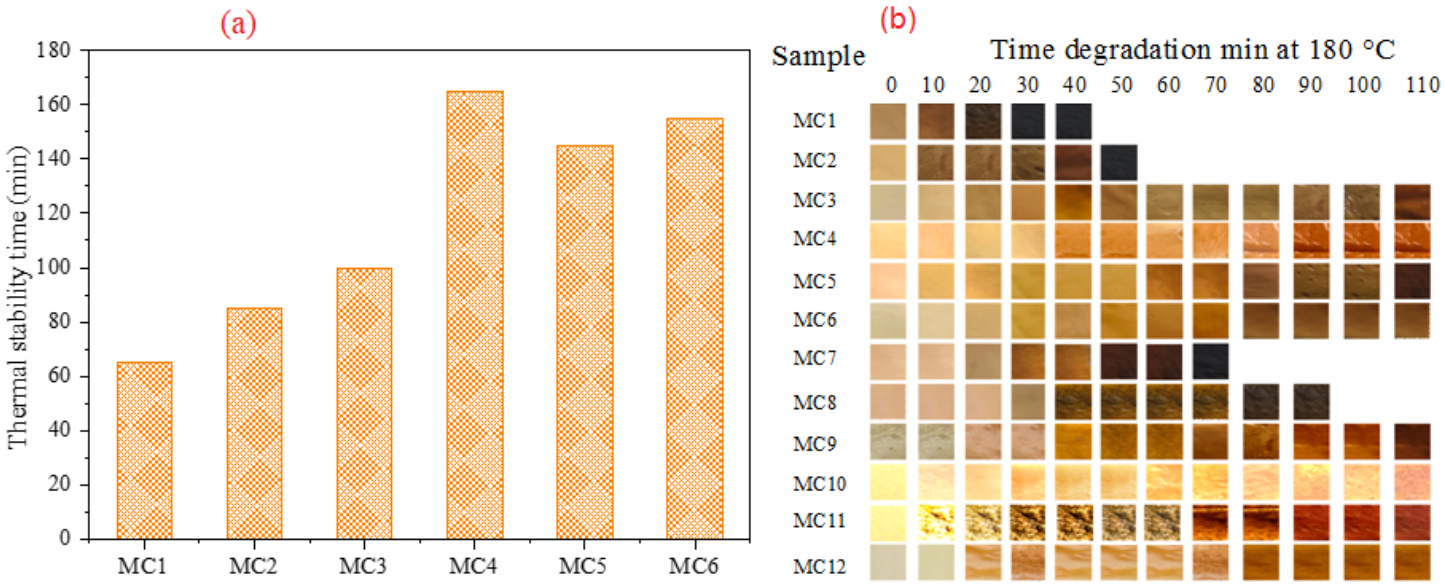

Figure 4

(a) Thermal stability time (Congo red test) of PVC microcomposites at 180°C. (b) Discoloration photos of PVC and PVC/r-LDPE microcomposites at 180°C for 110 min

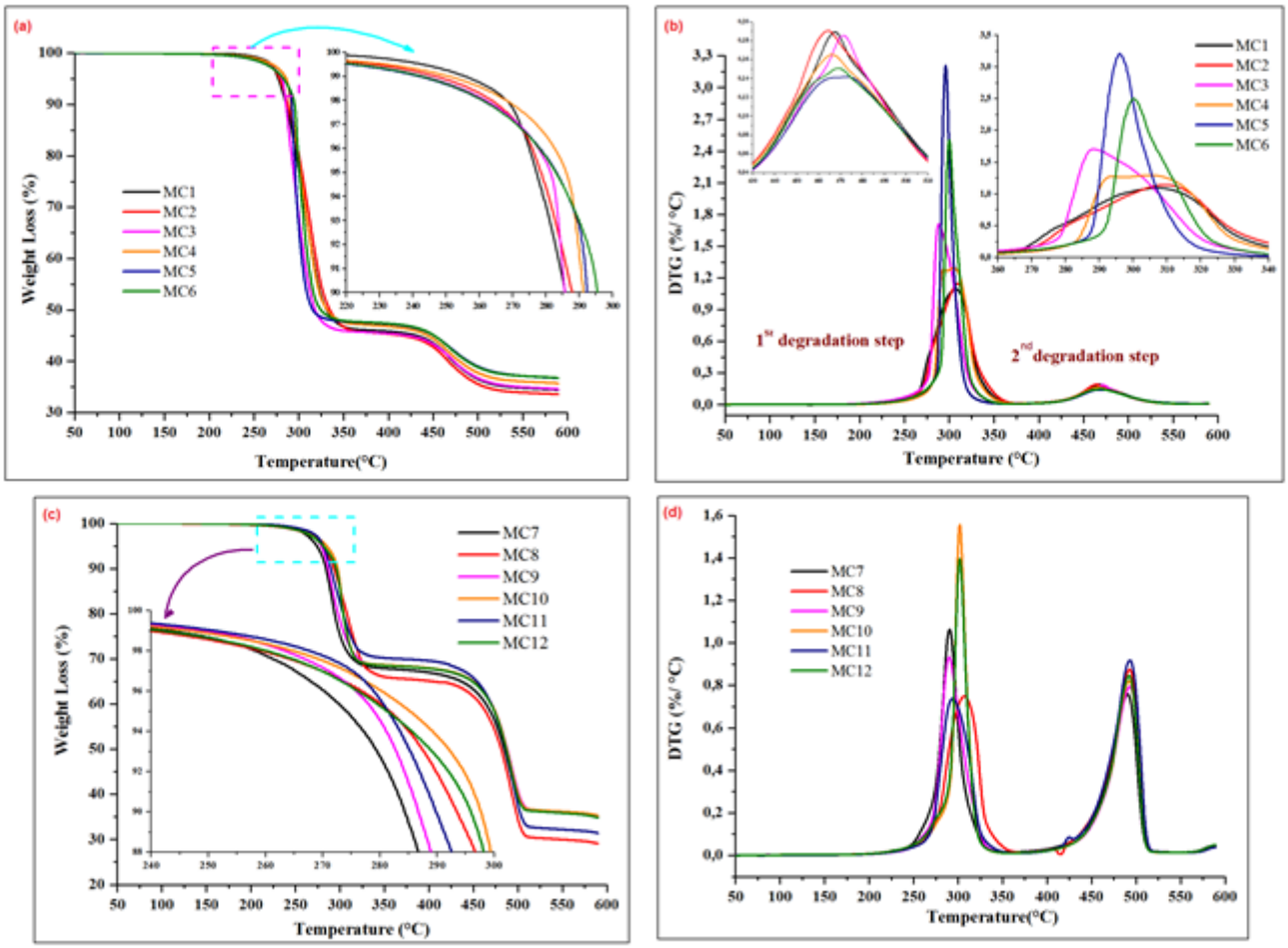

Figure 5

(a, b) TGA and DTG curves of PVC and (c, d) TGA and DTG curves of PVC/r-LDPE microcomposites

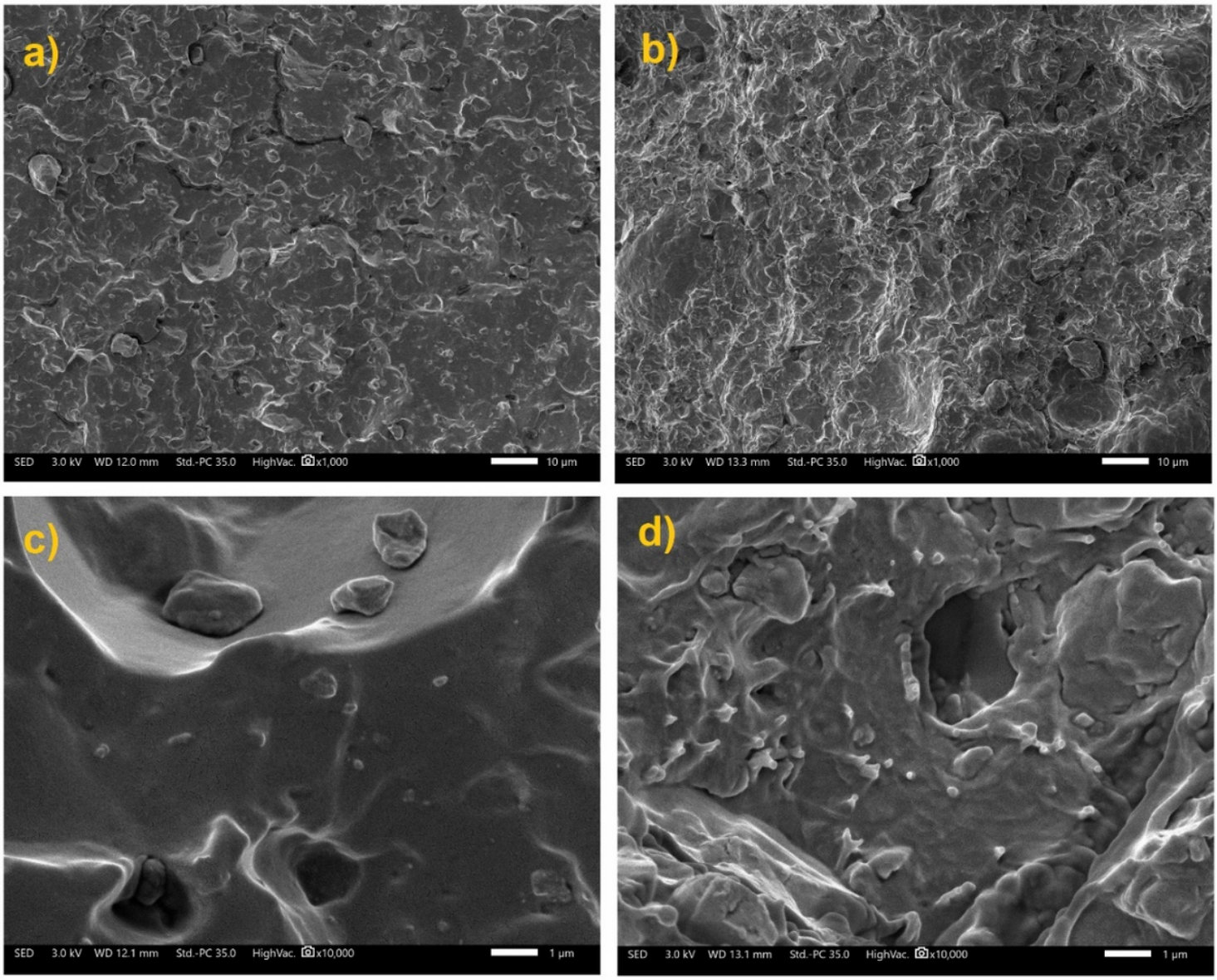

Figure 6

SEM images of the fracture surfaces of (a,c) MC4 and (b,d) MC10 microcomposites

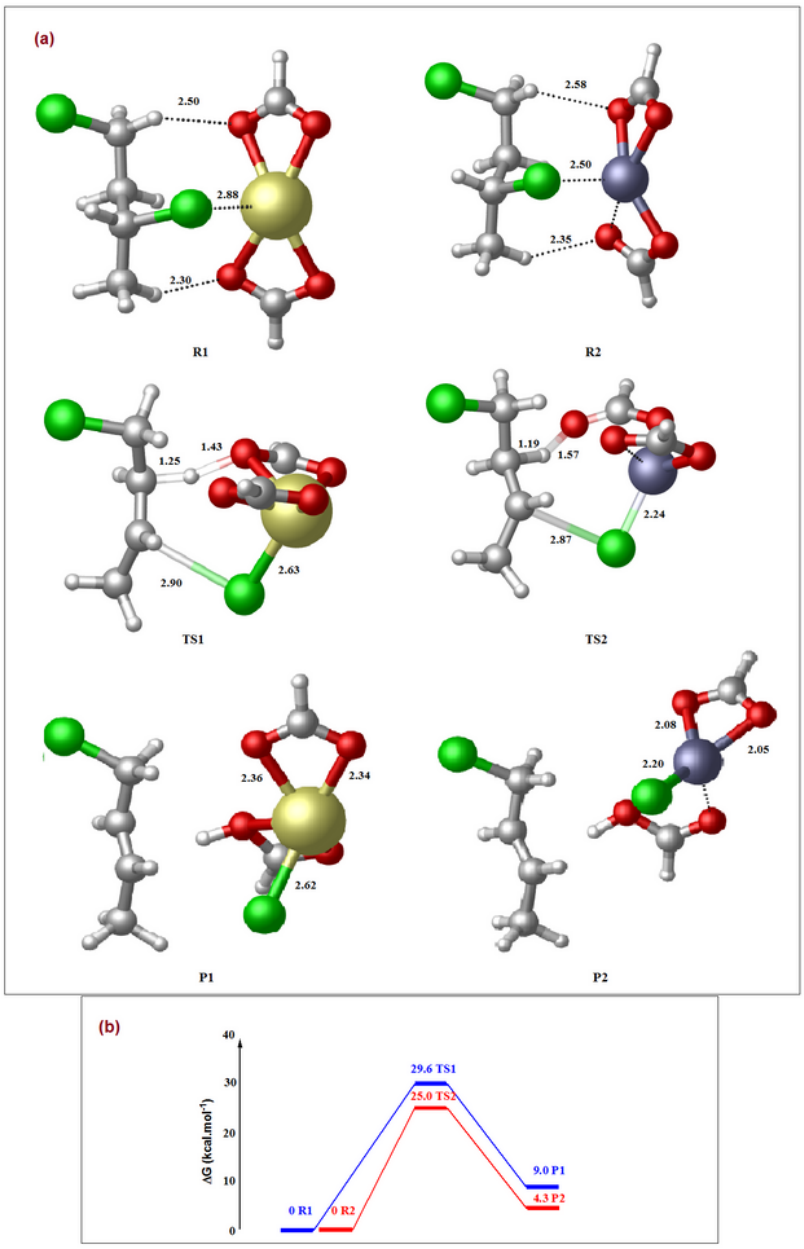

Figure 7

(a) Optimized geometries of reactants, transition states and products for the thermal dehydrochlorination of PVC with different thermal stabilizers. Distance given in A°.Atom color code: H in white, C in grey, Cl in green, O in red, Ca in yellow and Zn in blue and (b) Relative free energies of the dehydrochlorination process with (blue) $CaSt_2$ and (red) $ZnSt_2$ at the M06-2X/6-31++G(p,d) level

Supplementary Files

This is a list of supplementary files associated with this preprint. Click to download.

- GRAPHICALABSTRACT.tif